Real-Time Investigation of Lung Surfactant Respreading with Surface Vibrational Spectroscopy

ARTICLE *in* LANGMUIR · JANUARY 2007

Impact Factor: 4.46 · DOI: 10.1021/la061476k · Source: PubMed

2 AUTHORS, INCLUDING:

Heather C Allen
The Ohio State University
126 PUBLICATIONS **3,394** CITATIONS

Real-Time Investigation of Lung Surfactant Respreading with Surface Vibrational Spectroscopy

Gang Ma and Heather C. Allen*

Department of Chemistry, The Ohio State University, 100 West 18th Avenue, Columbus, Ohio 43210

Received May 24, 2006. In Final Form: September 22, 2006

The respreading of a lung surfactant monolayer at the air−water interface is investigated with broad bandwidth sum frequency generation (BBSFG) spectroscopy. The lung surfactant mixture contains chain perdeuterated dipalmitoylphosphatidylcholine (DPPC-d_{62}), palmitoyloleoylphosphatidylglycerol (POPG), palmitic acid (PA), and KL_4 (a 21-residue polypeptide analogue to the surfactant protein SP-B). DPPC-d_{62} serves as a probe molecule for the spectroscopic investigation. The BBSFG spectra of DPPC-d_{62} in the lung surfactant mixture are obtained in the C−D stretching region in real-time during film compression and expansion in a Langmuir trough. The BBSFG intensity of the CD_3 stretch peak from DPPC-d_{62} terminal methyl groups is used as a measure of the interfacial density of DPPC-d_{62} after careful consideration of orientation effects. For the first time, the interfacial loss of DPPC in a complex lung surfactant mixture is quantified. Spectroscopic results reveal that there is an 18% DPPC-d_{62} interfacial loss during film respreading. However, the surface pressure−area isotherm measurements demonstrate that there is a rather large trough area reduction (37%) during film expansion. The relatively small interfacial loss of DPPC-d_{62} and the rather large trough area reduction indicate that the respreading of DPPC and non-DPPC components in the lung surfactant is not uniform and a surface refinement process exists during film compression and expansion. This refinement process results in a DPPC-enriched monolayer with a significant depletion of non-DPPC components after film respreading. Implication for replacement surfactant design from this work is discussed.

Introduction

Lung surfactant lipids and proteins assemble at the air−alveolus interface, forming a monolayer on the alveolar hypophase. The surfactant mixture lowers the surface tension at the alveolar surface to near-zero values during the breathing cycle and is crucial for proper function of the lung.[1,2] Respiratory distress syndrome (RDS), a lung disorder due to a deficiency of lung surfactant, affects tens of thousands of premature infants every year.[2] The use of exogenous surfactants is a currently accepted treatment for this deficiency.[3] Thus, design of more effective exogenous surfactants is a critically important area of lung surfactant research.

The endogenous lung surfactant contains about 90 wt % lipids and 10 wt % surfactant proteins.[4,5] Phospholipids, including phosphatidylcholine, phosphatidylglycerol, phosphatidylethanolamine, phosphatidylinositol, and phosphatidylserine, make up the majority of the lipid composition with dipalmitoylphosphatidylcholine (DPPC) being the major phospholipid component. In mammalian lung, 40 wt % of the total phospholipid is DPPC. There are four types of surfactant proteins, SP-A, SP-B, SP-C, and SP-D. Among them, SP-B has been considered as the most important protein. Deficiency of SP-B due to mutations in the SP-B gene will lead to lethal respiratory distress in either humans[6] or knock-out mice.[7]

Lung surfactant must possess three essential properties in order to function properly at the air−alveolus interface. It must be able to adsorb quickly from the hypophase to the air−water interface, it must be able to reach a near-zero surface tension value at the end of exhalation, and it must be able to respread at the air−water interface quickly during inhalation.[2] No single lung surfactant component has these three optimized properties. Therefore, lung surfactant must be a multicomponent functional mixture. As for the roles of lipids and proteins in lung surfactant, it is generally accepted that DPPC is responsible for the near-zero surface tension at the alveolar surface at the end of exhalation. Other lipids (e.g. unsaturated phospholipids, anionic phospholipids) and proteins (SP-B and SP-C) are believed to facilitate the respreading and adsorption of DPPC.[2,4,5]

Exogenous lung surfactants used in surfactant replacement therapy are not exact duplicates of their endogenous counterparts in the human lungs, but they have to carry the three essential properties mentioned above. So far, the most effective replacement surfactants are still animal-derived surfactant preparations, for example, Survanta.[2,8] Scientists have been working to develop synthetic surfactant preparations, also considered as the new generation of replacement surfactants. Promising candidates (e.g., Surfaxin, a synthetic peptide-based surfactant preparation) have emerged in recent years.[8,9]

In the past 30 years, numerous studies have been performed on lung surfactant monolayers with a variety of physiochemical approaches, including Langmuir film balance,[10−15] captive bubble apparatus,[16−18] pulsating bubble surfactometer,[19] fluores-

* Corresponding author. E-mail: allen@chemistry.ohio-state.edu.

(1) Goerke, J. *Biochim. Biophys. Acta* **1998**, *1408*, 79.
(2) Notter, R. H. *Lung Surfactants: Basic Science and Clinical Applications*; Marcel Dekker: New York, 2000.
(3) Robertson, B.; Halliday, H. L. *Biochim. Biophys. Acta* **1998**, *1408*, 346.
(4) Creuwels, L. A. J. M.; Van Golde, L. M. G.; Haagsman, H. P. *Lung* **1997**, *175*, 1.
(5) Veldhuizen, R.; Nag, K.; Orgeig, S.; Possmayer, F. *Biochim. Biophys. Acta* **1998**, *1408*, 90.
(6) Nogee, L. M.; Garnier, G.; Dietz, H. C.; Singer, L.; Murphy, A. M.; deMello, D. E.; Colten, H. R. *J. Clin. Invest.* **1994**, *93*, 1860.
(7) Tokieda, K.; Whitsett, J. A.; Clark, J. C.; Weaver, T. E.; Ikeda, K.; McConnell, K. B.; Jobe, A. H.; Ikegami, M.; Iwamoto, H. S. *Am. J. Physiol.* **1997**, *273*, L875.
(8) Pfister, R. H.; Soll, R. F. *Biol. Neonate* **2005**, *87*, 338.
(9) Cochrane, C. G.; Revak, S. D. *Science* **1991**, *254*, 566.
(10) Notter, R. H.; Tabak, S. A.; Mavis, R. D. *J. Lipid Res.* **1980**, *21*, 10.
(11) Fleming, B. D.; Keough, K. M. W. *Chem. Phys. Lipids* **1988**, *49*, 81.
(12) Longo, M. L.; Bisagno, A. M.; Zasadzinski, J. A.; Bruni, R.; Waring, A. J. *Science* **1993**, *261*, 453.
(13) Taneva, S. G.; Keough, K. M. W. *Biochemistry* **1994**, *33*, 14660.
(14) Wang, Z.; Hall, S. B.; Notter, R. H. *J. Lipid Res.* **1995**, *36*, 1283.
(15) Ma, J.; Koppenol, S.; Yu, H.; Zografi, G. *Biophys. J.* **1998**, *74*, 1899.
(16) Schurch, S.; Green, F. H.; Bachofen, H. *Biochim. Biophys. Acta* **1998**, *1408*, 180.
(17) Zuo, Y. Y.; Gitiafroz, R.; Acosta, E.; Policova, Z.; Cox, P. N.; Hair, M. L.; Neumann, A. W. *Langmuir* **2005**, *21*, 10593.

10.1021/la061476k CCC: $33.50
Published on Web 11/23/2006

cence microscopy (FM),[15,20−29] Brewster angle microscopy (BAM),[21,23,25,28−31] atomic force microscopy (AFM),[26,27,29,31,32] grazing incidence X-ray diffraction (GIXD),[29,30,33,34] infrared reflection−absorption spectroscopy (IRRAS),[35−40] sum frequency generation spectroscopy,[41] and computer simulation.[42,43] Langmuir monolayers are frequently chosen model systems in the in vitro lung surfactant fundamental research.[2,44] The film compression and expansion processes can be considered as mimics of exhalation and inhalation processes.

The present study focuses on the respreading process of a lung surfactant Langmuir monolayer at the air−water interface. Respreading is a process by which surfactant molecules that are ejected into interfacial aggregates of the collapse phases during compression are able to reenter and spread back into the film during expansion.[2] Respreading is related to the interfacial surfactant loss. Good respreading means less interfacial surfactant loss, which is crucial to keep lung surfactant from being depleted during the breathing cycle. During the respreading of the multicomponent lung surfactant monolayer, components may not be in the same compositional ratio as in the original film. Or in other words, a surface refinement process can occur.[2] The respreading properties of a lung surfactant monolayer is believed to depend on surfactant molecular structures and intermolecular interactions.[10,11,13,14,24,26,27,31,39,45−49] For a single-component monolayer, Liu et al. investigated the respreading properties of a variety of phospholipids and phopspholipid analogues and found that even relatively small changes in molecular structures and headgroup charge could cause significant respreading property variations.[45,46] In a mixed monolayer, intermolecular interaction becomes a crucial factor affecting the film respreading properties. For example, Notter et al. found that adding dioleoylphosphatidylcholine or cholesterol could improve the respreading of DPPC in the binary lung surfactant film.[10] More recently, the possible role of surfactant proteins (SP-B and SP-C) in the respreading of complex lung surfactant monolayers has been explored.[13,14,24,26,27,31,39,47,48] Zasadzinski and co-workers have demonstrated with FM, BAM, and AFM that surfactant proteins can induce the formation of surface-associated structures by interacting with phospholipids.[24,26,27,31] These surface-associated structures can trap phospholipids (especially unsaturated and anionic phosphatidylglycerols) underneath the surface, preventing the irreversible surfactant loss into the subphase and, consequently, improve the respreading of phospholipids during film expansion.

A critical issue in lung surfactant respreading studies is the quantification of individual component's interfacial loss during film compression and expansion. However, there is a lack of methodology to deal with this issue. In previous studies, Notter and co-workers used the length ratio of the collapse phase plateau between the second and the first compression isotherms to evaluate the respreading of lung surfactant monolayers.[2,10,45,46] The bigger the ratio, the more efficient the repsreading. Yet, this method is not molecularly selective and it can be problematic when investigating complex lung surfactant mixtures. In this study, a molecularly selective method, vibrational sum frequency generation (VSFG) spectroscopy, is utilized to evaluate the respreading of DPPC in a complex lung surfactant system, quantitatively. The complex lung surfactant system employed in this study is a four-component lung surfactant monolayer, containing DPPC, palmitoyloleoylphosphatidylglycerol (POPG), palmitic acid (PA), and KL_4 (a 21-residue polypeptide serving as an analogue to SP-B). These four components are the only four ingredients used in the synthetic replacement surfactant Surfaxin, a new-generation surfactant mixture.[2,8] Respreading of KL_4 systems has not been previously investigated. Understanding the interfacial properties of this novel lung surfactant mixture has obvious relevance for surfactant replacement therapy.

VSFG spectroscopy is a surface-selective vibrational spectroscopy technique and has been widely used to study the interfacial properties of Langmuir monolayers[41,50−58] and Lang-

(18) Smith, E. C.; Crane, J. M.; Laderas, T. G.; Hall, S. B. *Biophys. J.* **2003**, *85*, 3048.
(19) Chang, C.-H.; Coltharp, K. A.; Park, S. Y.; Franses, E. I. *Colloids Surf., A* **1996**, *114*, 185.
(20) Nag, K.; Perez-Gil, J.; Cruz, A.; Keough, K. M. W. *Biophys. J.* **1996**, *71*, 246.
(21) Discher, B. M.; Maloney, K. M.; Schief, W. R.; Grainger, D. W.; Vogel, V.; Hall, S. B. *Biophys. J.* **1996**, *71*, 2583.
(22) Kruger, P.; Schalke, M.; Wang, Z.; Notter, R. H.; Dluhy, R. A.; Losche, M. *Biophys. J.* **1999**, *77*, 903.
(23) Lipp, M. M.; Lee, K. Y. C.; Zasadzinski, J. A.; Waring, A. J. *Rev. Sci. Instrum.* **1997**, *68*, 2574.
(24) Lipp, M. M.; Lee, K. Y. C.; Takamoto, D. Y.; Zasadzinski, J. A.; Waring, A. J. *Phys. Rev. Lett.* **1998**, *81*, 1650.
(25) Piknova, B.; Schief, W. R.; Vogel, V.; Discher, B. M.; Hall, S. B. *Biophys. J.* **2001**, *81*, 2172.
(26) Ding, J.; Takamoto, D. Y.; von Nahmen, A.; Lipp, M. M.; Lee, K. Y. C.; Waring, A. J.; Zasadzinski, J. A. *Biophys. J.* **2001**, *80*, 2262.
(27) Takamoto, D. Y.; Lipp, M. M.; von Nahmen, A.; Lee, K. Y. C.; Waring, A. J.; Zasadzinski, J. A. *Biophys. J.* **2001**, *81*, 153.
(28) Schief, W. R.; Antia, M.; Discher, B. M.; Hall, S. B.; Vogel, V. *Biophys. J.* **2003**, *84*, 3792.
(29) Alonso, C.; Alig, T.; Yoon, J.; Bringezu, F.; Warriner, H.; Zasadzinski, J. A. *Biophys. J.* **2004**, *87*, 4188.
(30) Bringezu, F.; Ding, J.; Brezesinski, G.; Waring, A. J.; Zasadzinski, J. A. *Langmuir* **2002**, *18*, 2319.
(31) Ding, J.; Doudevski, I.; Warriner, H. E.; Alig, T.; Zasadzinski, J. A.; Waring, A. J.; Sherman, M. A. *Langmuir* **2003**, *19*, 1539.
(32) Flanders, B. N.; Vickery, S. A.; Dunn, R. C. *J. Microsc.* **2001**, *202*, 379.
(33) Lee, K. Y. C.; Gopal, A.; von Nahmen, A.; Zasadzinski, J. A.; Majewski, J.; Smith, G. S.; Howes, P. B.; Kjaer, K. *J. Chem. Phys.* **2002**, *116*, 774.
(34) Lee, K. Y. C.; Majewski, J.; Kuhl, T. L.; Howes, P. B.; Kjaer, K.; Lipp, M. M.; Waring, A. J.; Zasadzinski, J. A.; Smith, G. S. *Biophys. J.* **2001**, *81*, 572.
(35) Dluhy, R. A.; Reilly, K. E.; Hunt, R. D.; Mitchell, M. L.; Mautone, A. J.; Mendelsohn, R. *Biophys. J.* **1989**, *56*, 1173.
(36) Pastrana-Rios, B.; Flach, C. R.; Brauner, J. W.; Mautone, A. J.; Mendelsohn, R. *Biochemistry* **1994**, *33*, 5121.
(37) Pastrana-Rios, B.; Taneva, S.; Keough, K. M. W.; Mautone, A. J.; Mendelsohn, R. *Biophys. J.* **1995**, *69*, 2531.
(38) Cai, P.; Flach, C. R.; Mendelsohn, R. *Biochemistry* **2003**, *42*, 9446.
(39) Wang, L.; Cai, P.; Galla, H.-J.; He, H.; Flach, C. R.; Mendelsohn, R. *Eur. Biophys. J.* **2005**, *34*, 243.
(40) Shanmukh, S.; Biswas, N.; Waring, A. J.; Walther, F. J.; Wang, Z.; Chang, Y.; Notter, R. H.; Dluhy, R. A. *Biophys. Chem.* **2005**, *113*, 233.
(41) Ma, G.; Allen, H. C. *Langmuir* **2006**, *22*, 5341.
(42) Kaznessis, Y. N.; Larson, R. G. In *Lung Surfactant Function and Disorder*; Nag, K., Ed.; Taylor & Francis Group: Boca Raton, FL, 2005; p 229.
(43) Freites, J. A.; Choi, Y.; Tobias, D. J. *Biophys. J.* **2003**, *84*, 2169.
(44) Zasadzinski, J. A.; Ding, J.; Warriner, H. E.; Bringezu, F.; Waring, A. J. *Curr. Opin. Colloid Interface Sci.* **2001**, *6*, 506.
(45) Liu, H.; Turcotte, J. G.; Notter, R. H. *J. Colloid Interface Sci.* **1994**, *167*, 391.
(46) Liu, H.; Lu, R. Z.; Turcotte, J. G.; Notter, R. H. *J. Colloid Interface Sci.* **1994**, *167*, 378.
(47) von Nahmen, A.; Schenk, M.; Sieber, M.; Amrein, M. *Biophys. J.* **1997**, *72*, 463.
(48) Krol, S.; Ross, M.; Sieber, M.; Kunneke, S.; Galla, H.-J.; Janshoff, A. *Biophys. J.* **2000**, *79*, 904.
(49) Chang, Y.; Wang, Z.; Schwan, A. L.; Wang, Z.; Holm, B. A.; Baatz, J. E.; Notter, R. H. *Chem. Phys. Lipids* **2005**, *137*, 77.
(50) Guyot-Sionnest, P.; Hunt, J. H.; Shen, Y. R. *Phys. Rev. Lett.* **1987**, *59*, 1597.
(51) Zhang, D.; Gutow, J.; Eisenthal, K. B. *J. Phys. Chem.* **1994**, *98*, 13729.
(52) Walker, R. A.; Gruetzmacher, J. A.; Richmond, G. L. *J. Am. Chem. Soc.* **1998**, *120*, 6991.
(53) Zhuang, X.; Miranda, P. B.; Kim, D.; Shen, Y. R. *Phys. Rev. B* **1999**, *59*, 12632.
(54) Gurau, M. C.; Castellana, E. T.; Albertorio, F.; Kataoka, S.; Lim, S.-M.; Yang, R. D.; Cremer, P. S. *J. Am. Chem. Soc.* **2003**, *125*, 11166.
(55) Roke, S.; Schins, J.; Muller, M.; Bonn, M. *Phys. Rev. Lett.* **2003**, *90*, 128101/1.
(56) Watry, M. R.; Tarbuck, T. L.; Richmond, G. L. *J. Phys. Chem. B* **2003**, *107*, 512.
(57) Nickolov, Z. S.; Britt, D. W.; Miller, J. D. *J. Phys. Chem. B* **2006**, *110*, 15506.
(58) Voss, L. F.; Hadad, C. M.; Allen, H. C. *J. Phys. Chem. B* **2006**, *110*, 19487.

muir−Blodgett films.[59−66] In this study, VSFG spectroscopy is utilized in real-time by taking snapshot spectra during film compression and expansion to address the dynamic nature of lung surfactant monolayer respreading. The basic approach is to use VSFG spectroscopy to gain information about the surface molecular density variation of surfactant components during film respreading. The density variation can then be used to evaluate the respreading process. Chain perdeuterated DPPC (DPPC-d_{62}) is used in the lung surfactant mixture to overcome the vibrational frequency overlap. In this way, the surface molecular density of DPPC-d_{62} can be specifically tracked by VSFG spectroscopy. By combining the VSFG spectroscopic technique and compression−expansion isotherm measurements, a surface refinement process during film respreading is revealed. Due to the surface refinement process, the lung surfactant film after film respreading becomes relatively enriched in DPPC as compared with the original film.

VSFG is a second-order nonlinear process. VSFG spectra are obtained by probing the surface with two pulsed lasers, one in the visible spectral region and the other in the infrared spectral region. A surface second-order response is generated at a third frequency, the sum of the two probing beams' frequencies. When the infrared pulse is resonant with a vibrational mode of the molecule adsorbed at the surface, there will be an SFG signal enhancement. The SFG signal is derived from the Raman scattering response from an infrared excited mode. Thus, it is related to Raman and infrared spectroscopies but is unique in its selection rules. SFG requires a lack of inversion symmetry and the vibrational mode probed must be Raman- and IR-active. These selection rules make SFG surface selective and also highly sensitive to surface molecular alignment. SFG spectra appear simplified relative to infrared spectra due to these selection rules, in particular, the need for a lack of inversion symmetry. There are two types of VSFG technologies: scanning VSFG and broad bandwidth VSFG (BBSFG). In this study, BBSFG technology is used.

Brielfly, VSFG is outlined here. Details can be found in the literature.[53,67−71] The VSFG intensity, I_{SFG}, as shown in eq 1,

$$I_{SFG} \propto |\chi^{(2)}|^2 \propto |\chi_{NR}{}^{(2)} + \sum_{\upsilon} \chi_{\upsilon}{}^{(2)}|^2 \quad (1)$$

is proportional to the absolute square of the macroscopic second-order susceptibility, $\chi^{(2)}$, which consists of resonant terms ($\chi_{\upsilon}{}^{(2)}$) and a nonresonant term ($\chi_{NR}{}^{(2)}$). When the frequency of an incident infrared beam, ω_{IR}, is resonant with a vibrational mode, υ, at the surface, the resonant susceptibility term ($\chi_{\upsilon}{}^{(2)}$) dominates the nonlinear susceptibility ($\chi^{(2)}$) and an SFG intensity enhancement is observed. The resonant macroscopic nonlinear susceptibility, $\chi_{\upsilon}{}^{(2)}$, is shown in eq 2,

$$\chi_{\upsilon}{}^{(2)} \propto \frac{A_{\upsilon}}{\omega_{IR} - \omega_{\upsilon} + i\Gamma_{\upsilon}} \quad (2)$$

where A_{υ} is the strength of the transition moment, ω_{υ} is the frequency of the transition moment, and Γ_{υ} describes the linewidth of the transition. The strength, A_{υ}, is nonzero when the Raman and the infrared transitions are spectroscopically allowed. $\chi_{\upsilon}{}^{(2)}$ is related to the molecular hyperpolarizability, β_{υ}, shown in eq 3,

$$\chi_{\upsilon}{}^{(2)} = N\sum_{lmn} \langle \mu_{IJK:lmn} \rangle \beta_{\upsilon} \quad (3)$$

by the molecular density of the surface species, N, and an orientationally averaged Euler angle transformation, $\langle \mu_{IJK:lmn} \rangle$, between the laboratory coordinates (I, J, K) and the molecule coordinates (l, m, n). The Euler angle transformation contains the molecular orientation information.

Experimental Section

Materials. Acyl chain deuterated 1,2-dipalmitoyl-*sn*-glycero-3-phosphocholine (DPPC-d_{62}) and 1-palmitoyl-2-oleoyl-*sn*-glycero-3-phosphatidylglycerol (POPG) were purchased from Avanti Polar Lipids (Alabaster, AL) with >99% purity. Palmitic acid (PA) with a 99% purity was purchased from Sigma-Aldrich. The KL_4 peptide with an amino acid sequence of KLLLLKLLLLKLLLLKLLLLK (K, lysine; L, leucine) was custom synthesized by Biopeptide Co., LLC (San Diego, CA) with a purity of 98% by HPLC.

EDTA, Trizma [tris(hydroxymethyl) aminomethane base], hydrochloric acid, and sodium chloride were obtained from Fisher Scientific. Spectrophotometric grade chloroform and methanol were purchased from Sigma-Aldrich. Deionized water was from a Barnstead Nanopure system with a resistivity of 18.2 MΩ·cm.

Sample Preparation. A stock solution of DPPC-d_{62} with a concentration of 1 mM was made in chloroform, a stock solution of POPG with a concentration of 1 mM was made in chloroform/methanol (3/1 v/v), a stock solution of PA with a concentration of 1 mM was made in chloroform, and a stock solution of KL_4 with a concentration of 0.65 mg/mL was made in chloroform/methanol (3/1 v/v). These four stock solutions were mixed in appropriate ratios to form a lung surfactant mixture with a formula of DPPC-d_{62}/POPG/PA/KL_4 = 66/22/7/5 by weight. This formula is similar to the formula used in previous lung surfactant studies.[9,72] The subphase used in monolayer measurements is an aqueous solution consisting of 100 mM NaCl and 0.1 mM EDTA in 5 mM Tris buffer at pH = 7.[38]

Methods. *Langmuir Film Balance.* The monolayer compression and expansion were performed in a Langmuir trough (KSV minitrough, KSV). The rectangular trough (176.5 mm × 85 mm) is made of Teflon and was thermostated by circulating water in channels placed underneath the trough at a temperature of 24 ± 0.5 °C. Two barriers were employed to provide symmetric film compression. The barriers are made of Delrin, which prevents leakage of the monolayer beneath the barriers. The surface pressure and the mean molecular area (or trough area) were continuously monitored during film compression and expansion by the Wilhelmy plate method. The plate was necessarily made of filter paper. The trough was filled with buffer solution as the subphase. A known amount of the lung surfactant mixture solution was spread on the buffer subphase in a dropwise manner with a Hamilton syringe, and 10 min was allowed to elapse for complete solvent evaporation before starting the compression. The same barrier moving speeds (5 mm/min per barrier) were used for both film compression and expansion. Expansion followed directly after the compression was finished. To

(59) Akamatsu, N.; Domen, K.; Hirose, C.; Onishi, T.; Shimizu, H.; Masutani, K. *Chem. Phys. Lett.* **1991**, *181*, 175.
(60) Akamatsu, N.; Domen, K.; Hirose, C. *J. Phys. Chem.* **1993**, *97*, 10070.
(61) Du, Q.; Xiao, X. D.; Charych, D.; Wolf, F.; Frantz, P.; Shen, Y. R.; Salmeron, M. *Phys. Rev. B* **1995**, *51*, 7456.
(62) Fraenkel, R.; Butterworth, G. E.; Bain, C. D. *J. Am. Chem. Soc.* **1998**, *120*, 203.
(63) Liu, J.; Conboy, J. C. *J. Am. Chem. Soc.* **2004**, *126*, 8376.
(64) Liu, J.; Conboy, J. C. *J. Am. Chem. Soc.* **2004**, *126*, 8894.
(65) Ye, S.; Noda, H.; Nishida, T.; Morita, S.; Osawa, M. *Langmuir* **2004**, *20*, 357.
(66) Holman, J.; Davies, P. B.; Nishida, T.; Ye, S.; Neivandt, D. J. *J. Phys. Chem. B* **2005**, *109*, 18723.
(67) Hirose, C.; Akamatsu, N.; Domen, K. *Appl. Spectrosc.* **1992**, *46*, 1051.
(68) Moad, A. J.; Simpson, G. J. *J. Phys. Chem. B* **2004**, *108*, 3548.
(69) Wang, J.; Clarke, M. L.; Chen, Z. *Anal. Chem.* **2004**, *76*, 2159.
(70) Wang, H.-F.; Gan, W.; Lu, R.; Rao, Y.; Wu, B.-H. *Int. Rev. Phys. Chem.* **2005**, *24*, 191.
(71) Lambert, A. G.; Davies, P. B.; Neivandt, D. J. *Appl. Spectrosc. Rev.* **2005**, *40*, 103.
(72) Palmblad, M.; Gustafsson, M.; Curstedt, T.; Johansson, J.; Schurch, S. *Biochim. Biophys. Acta* **2001**, *1510*, 106.

Scheme 1. The BBSFG Experiment on a Langmuir Trough

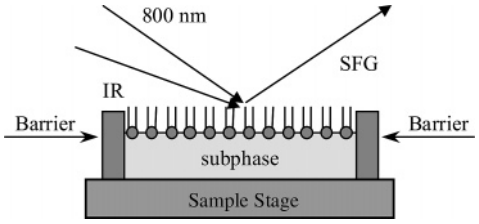

address the concern that the unsaturated lipid (POPG has one C=C bond on its oleic acid chain) may be oxidized by atmospheric oxidants,[73] the trough system was enclosed in a N_2-purged plastic chamber. Two tube inlets carry nitrogen gas into the chamber for continuous purging during measurements. Experiments under ambient atmospheric conditions were also performed and are included in the Supporting Information. No significant difference was found between the results obtained under these two conditions (N_2-purging versus ambient atmosphere).

Broad Bandwidth Sum Frequency Generation Laser System. The BBSFG laser system consists of two 1-kHz repetition rate regenerative amplifiers (Spectra-Physics Spitfire, fs and ps versions), both of which are seeded by sub-50-fs, 792-nm pulses (the wavelength is tuned for system optimization) from a Ti:sapphire oscillator (Spectra-Physics, Tsunami) and pumped by a 527-nm beam from an all solid-state Nd:YLF laser (Spectra-Physics, Evolution 30). The two regenerative amplifiers provide 85-fs pulses at 800 nm (22 nm bandwidth) and 2-ps pulses at 800 nm (17 cm^{-1} bandwidth). The femtosecond broad bandwidth pulses are then used to generate broad bandwidth infrared light via an optical parametric amplifier (Spectra-Physics, OPA-800CF). The spectral window of the broad IR pulse can be as large as 500 cm^{-1}, depending on the tuned spectral region. Therefore, using a BBSFG system, a surface vibrational spectrum can be obtained without wavelength scanning. In this work, the output energy of each 800-nm, ps pulse was 400 μJ, and the IR energies in the C−D and C−H stretching regions were 6 μJ per pulse and 7 μJ per pulse, respectively. As shown in Scheme 1, the Langmuir film balance was placed on the sample stage of the BBSFG system. The 800-nm, ps beam and the spectrally broad IR beam were overlapped at the monolayer surface spatially and temporally. The generated SFG signal containing spectral information from the monolayer was detected using a monochromator−CCD detection system (Acton Research, SpectraPro SP-500 monochromator with a 1200 g/mm grating blazed at 750 nm; Roper Scientific, 1340 × 400 pixel array, LN400EB back-illuminated CCD).

The SFG spectrum is polarization dependent. In this study, the polarization combination of ssp (s-SFG, s-800 nm, p-infrared) was used. The SFG spectrum was normalized against a nonresonant SFG spectrum from a GaAs crystal (Lambda Precision Optics, Inc) to remove the spectral distortion caused by the energy profile of the infrared pulse. To calibrate the SFG peak positions, a nonresonant SFG spectrum from the GaAs crystal surface was obtained with a polystyrene film covering the OPA infrared output port. The resulting SFG spectrum containing polystyrene infrared absorption bands was used for the calibration. The calibration accuracy is better than 1 cm^{-1}.

The BBSFG system combined with the Langmuir film balance can work in three different modes: pause mode, hold mode, and real-time mode. In pause mode, the barriers compress the monolayer to a given surface pressure and halt and a BBSFG spectrum is then taken during the halting period. In hold mode, the barriers move to hold the surface pressure at a given value and a BBSFG spectrum is then taken during the holding period. In this study, the real-time mode was adopted. With the real-time mode, the BBSFG spectra were taken simultaneously during film compression and expansion. Therefore, each spectrum covers a segment of the isotherm. In this work, it takes 876 s to finish film compression and another 876 s to finish film expansion. With a 29.2-s acquisition time, 60 BBSFG spectra cover the entire compression and expansion cycle.

(73) Gaines, G. L. *Insoluble Monolayers at Liquid−Gas Interfaces*; Interscience Publishers: New York, 1966.

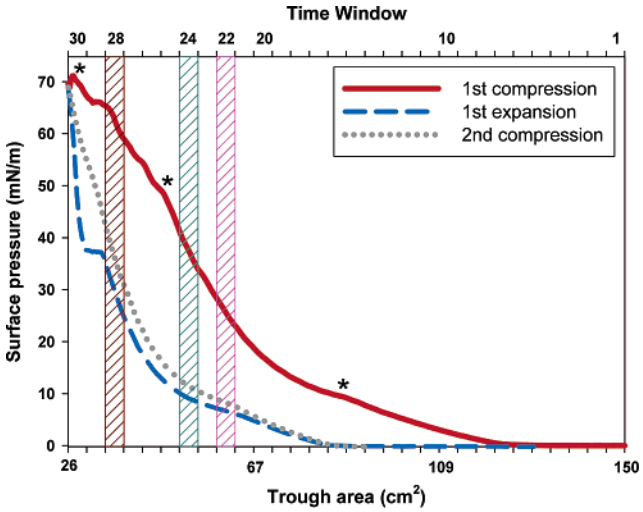

Figure 1. Compression and expansion isotherms of the DPPC-d_{62}−POPG−PA−KL_4 monolayer under N_2-purging conditions. The red curve is the first compression isotherm, the blue curve is the first expansion isotherm, the gray curve is the second compression isotherm, and the vertical columns are the three representative time windows. (The variability in the first compression curve between time windows #25 and #28 are not kinks.)

Results and Discussion

Figure 1 shows the compression and expansion isotherms of a DPPC−POPG−PA−KL_4 Langmuir monolayer at a temperature of 24 °C. The compression isotherm shows three major kinks as denoted by the three asterisks in Figure 1. Each kink corresponds to a phase transition. On the basis of previous investigations on multicomponent lung surfactant monolayers,[29] the first kink (from the far right of the compression isotherm) is due to a liquid-expanded to a liquid-condensed phase transition, the second kink is likely due to the collapse of the less stable component, such as POPG or KL_4, and the third kink is due to the collapse of DPPC.

A more obvious feature in Figure 1 is the existence of the hysteresis between the first compression isotherm and the first expansion isotherm. The hysteresis suggests surfactant loss at the interface during respreading, which represents ineffective film respreading.[2,13] If the monolayer has excellent respreading properties, the expansion curve would simply retrace the compression curve. However, when less surfactant respreads back into the film, the surface area occupied by lung surfactant molecules under the same surface pressure decreases as compared with that in the original film. Consequently, the expansion isotherm is shifted to the left with respect to the compression curve. As also shown in Figure 1, the second compression curve follows the first expansion curve very closely, further confirming that surfactant loss is the primary cause of the hysteresis during the first dynamic cycling.

Ideally, to investigate the respreading process of a mixed monolayer, we want to know the respreading properties of each individual component in the complex mixture. This type of information is extremely valuable for the precise engineering of synthetic replacement surfactant. However, as shown above, the monolayer isotherm measurement only provides one view about the overall effectiveness of the respreading of the lung surfactant monolayer. To overcome the limitation of this monolayer measurement technique, a surface spectroscopy technique, broad bandwidth sum frequency generation spectroscopy, is employed

in this study to gain further insight into the respreading process. In particular, we aim to explore two fundamental issues associated with the respreading process of a complex lung surfactant mixed monolayer. First, is the observed hysteresis primarily due to the significant interfacial material loss of DPPC? Second, does the monolayer, after film respreading, have the same composition as the original film?

The spectroscopic method utilized in this study is a real-time monitor of monolayer compression and expansion. As shown in Figure 1, the compression and expansion isotherms are divided into 30 segments (refer to the *x*-axis ticks), as denoted by the vertical columns in Figure 1. Segments are conveniently referred to as "time windows" (refer to the top *x*-axis label). The BBSFG spectra are taken simultaneously with the isotherm measurements. With a 29.2-s acquisition time, each BBSFG spectrum will cover one time window, giving spectroscopic information about each segment of the isotherm. Langmuir monolayers during dynamic compression and expansion are not at equilibrium, but are in metastable states. Due to the dynamic nature of the repsreading process, even a very short-period of barrier halting can significantly perturb the respreading process.[2] Therefore, it should be emphasized that a real-time approach is necessary to investigate film respreading.

The basic strategy of using BBSFG to investigate the respreading process is to use SFG to obtain interfacial density information about the surfactant component. Since in the same time window the monolayers during the compression process and the expansion process occupy the same trough area, the intensity variation of an individual component revealed from the BBSFG measurements will be directly related to the percentage of the interfacial net loss of the surfactant. In this study, deuterated DPPC (DPPC-d_{62}) is used as a spectroscopic probe to allow us to specifically track the interfacial density variation of DPPC-d_{62} during film compression and expansion.

Figure 2 shows the BBSFG spectra of DPPC-d_{62} during the first compression and the first expansion of the film in the three selected time windows: time window #22, time window #24, and time window #28. The six spectra shown in Figure 2 can be classified into two types, a spectrum having, or not having, CD_2-SS and CD_2-AS peaks. The frequencies and peak assignments of the fitted peaks are listed in Table 1. The peak assignments are also shown in Figure 2 with the vertical dashed lines. Peak assignments are based on previous infrared and Raman studies of deuterated DPPC.[74,75] The difference between the two types of spectra is due to the different DPPC-d_{62} interfacial structures. DPPC molecules have two distinct surface phases, the liquid-expanded (LE) phase and the liquid-condensed (LC) phase (also known as tilted-condensed phase).[76] In the LE phase, DPPC behaves like a two-dimensional liquid and its chains adopt gauche conformations. In the LC phase, DPPC behaves like a two-dimensional semicrystalline solid and its chains adopt an all-trans conformation. The selection rule of lack of inversion symmetry makes SFG very sensitive to the DPPC chain conformation. Methylene groups having gauche conformations within the DPPC chain will produce SFG signals at the methylene stretch frequencies. On the contrary, methylene groups in an all-trans conformation along the DPPC chain will not produce SFG signals at the methylene stretch frequencies, due to the existence of inversion symmetry within the pair of methylene groups (DPPC has an even number of methylene groups on each chain). For the time windows #22 and #24 in Figure 2A,B, the existence of the CD_2-SS and CD_2-AS vibrational intensities for the expansion segments demonstrates that DPPC-d_{62} is in the LE phase (or in the LE−LC coexistence region) during film

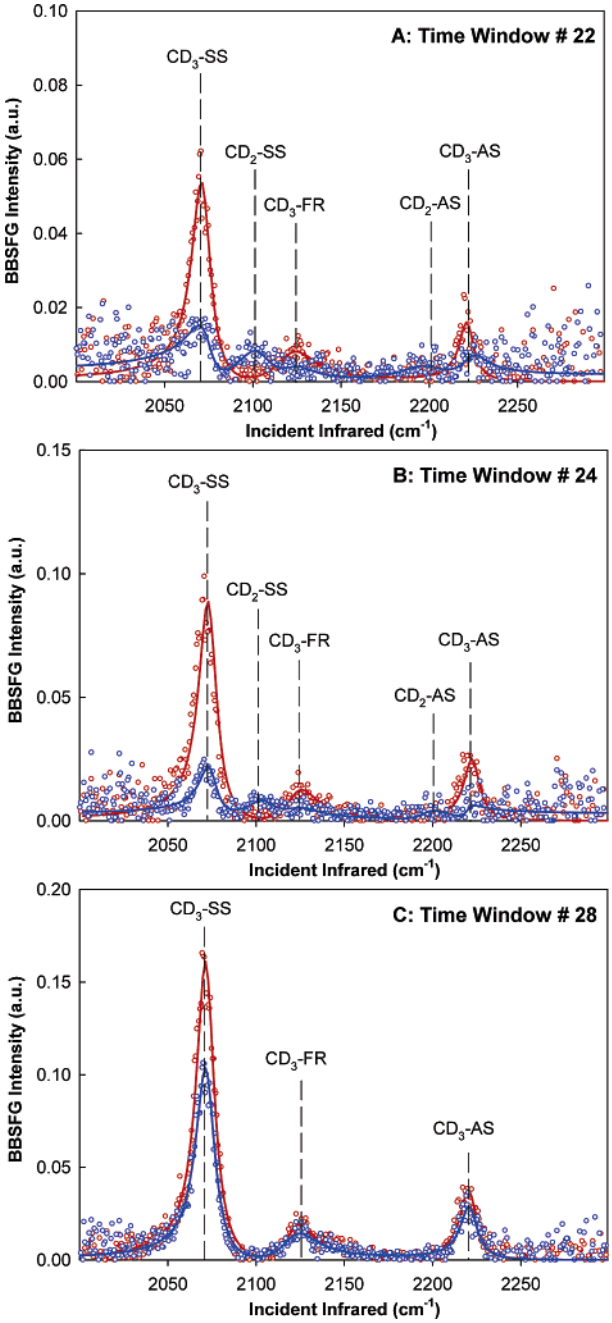

Figure 2. ssp BBSFG spectra of DPPC-d_{62} in DPPC-d_{62}−POPG−PA−KL_4 monolayer taken in the C−D stretching region in the three representative time windows under N_2-purging conditions. (A) time window #22, (B) time window #24, and (C) time window #28. Red spectra: spectra for the first compression isotherm segments. Blue spectra: spectra for the first expansion isotherm segments. Solid curves: spectral fits. CD_3-SS, CD_3 symmetric stretch; CD_2-SS, CD_2 symmetric stretch; CD_3-FR, CD_3 Fermi resonance; CD_2-AS, CD_2 asymmetric stretch; CD_3-AS, CD_3 asymmetric stretch.

Table 1. Fitted Peak Frequencies and Assignments of the BBSFG Spectra of DPPC-d_{62}[a]

CD_3-SS (cm^{-1})	CD_2-SS (cm^{-1})	CD_3-FR (cm^{-1})	CD_2-AS (cm^{-1})	CD_3-AS (cm^{-1})
2072	2102	2123	2200	2221

[a] SS, symmetric stretch; AS, asymmetric stretch; FR, Fermi resonance.

(74) Sunder, S.; Cameron, D. G.; Casal, H. L.; Boulanger, Y.; Mantsch, H. H. *Chem. Phys. Lipids* **1981**, *28*, 137.
(75) Devlin, M. T.; Levin, I. W. *J. Raman Spectrosc.* **1990**, *21*, 441.
(76) Kaganer, V. M.; Mohwald, H.; Dutta, P. *Rev. Mod. Phys.* **1999**, *71*, 779.

expansion. For the time window #28 in Figure 2C, the absence of CD_2-SS and CD_2-AS demonstrates that DPPC-d_{62} is in the LC phase during both compression and expansion.

As shown in Figure 2, in each of the three windows, an SFG intensity decrease is observed when comparing the spectrum of the compression segment and the spectrum of the expansion segment. The intensity decrease suggests that some surfactants are depleted from the air−water interface during film respreading. Although any peak in the spectra shown in Figure 2 could be potentially used as a measure of the surface density variation of DPPC-d_{62}, only the CD_3-SS peak is used as the measure of the interfacial density of DPPC-d_{62}. A practical reason is that the intensity of the CD_3-SS peak is much higher than other peaks.

As shown in eqs 1−3, the observed SFG intensity is a function of surface molecular density, surface molecular orientation, and the molecular hyperpolarizability. To be specific, with the ssp polarization combination measurement, the SFG intensity (I_{ssp}) of the CD_3-SS can be described in the following way, as shown in eq 4.[53]

$$\sqrt{I_{ssp}(CD_3\text{-SS})} \propto \chi_{yyz} = \frac{1}{2}N\beta_{ccc}[\langle\cos\theta\rangle(1+R) - \langle\cos^3\theta\rangle(1-R)] \quad (4)$$

In eq 4, I_{ssp} is the SFG intensity of the CD_3-SS peak, N is the interfacial density of the DPPC-d_{62}, β_{ccc} is the molecular hyperpolaribility, R is a ratio between the molecular hyperpolaribilities ($R = \beta_{aac}/\beta_{ccc}$), and θ is the orientation angle of the methyl group with respect to the surface normal. Since β_{ccc} and R are constants for a given system, the SFG intensity is a function of N and θ. However, the calculations of $\langle\cos\theta\rangle$ and $\langle\cos^3\theta\rangle$ are not necessarily straightforward and depend on the distribution function of the orientation angle θ. If the orientation angle θ has a Gaussian distribution, $\langle\cos\theta\rangle$ and $\langle\cos^3\theta\rangle$ will be written in the following forms (eqs 5−7), where θ_0 is the mean orientation angle and σ is a distribution factor.[77,78]

$$\langle\cos\theta\rangle = \frac{\int_0^\pi \cos\theta\, f(\theta)\sin\theta\, d\theta}{\int_0^\pi f(\theta)\sin\theta\, d\theta} \quad (5)$$

$$\langle\cos^3\theta\rangle = \frac{\int_0^\pi \cos^3\theta\, f(\theta)\sin\theta\, d\theta}{\int_0^\pi f(\theta)\sin\theta\, d\theta} \quad (6)$$

$$f(\theta) = \frac{1}{\sigma\sqrt{2\pi}}\exp[-(\theta-\theta_0)^2/(2\sigma^2)] \quad (7)$$

If a δ function can be assumed for the angle distribution function, $\langle\cos\theta\rangle$ and $\langle\cos^3\theta\rangle$ will be in a simplified form, as shown below (eqs 8 and 9).

$$\langle\cos\theta\rangle = \cos\theta \quad (8)$$

$$\langle\cos^3\theta\rangle = \cos^3\theta \quad (9)$$

In this way, eq 4 becomes eq 10.

$$\sqrt{I_{ssp}(CD_3\text{-SS})} \propto \chi_{yyz} = \frac{1}{2}N\beta_{ccc}[\cos\theta(1+R) - \cos^3\theta(1-R)] \quad (10)$$

(77) Wang, J.; Paszti, Z.; Even, M. A.; Chen, Z. *J. Am. Chem. Soc.* **2002**, *124*, 7016.

(78) Gan, W.; Wu, D.; Zhang, Z.; Feng, R.-R.; Wang, H.-F. *J. Chem. Phys.* **2006**, *124*, 114705.

Table 2. DPPC-d_{62} Interfacial Density Reduction ΔN versus Trough Area Reduction (ΔTA)

$I_{comp}(CD_3\text{-SS})^a$ (au)	$I_{expn}(CD_3\text{-SS})^b$ (au)	ΔN (%)	$TA_{comp-1st}{}^c$ (cm^2)	$TA_{expn-1st}{}^d$ (cm^2)	ΔTA (%)
2.92	1.94	18	59	37	37

[a] $I_{comp}(CD_3\text{-SS})$: peak intensity of CD_3-SS during film compression. [b] $I_{expn}(CD_3\text{-SS})$: peak intensity of CD_3-SS during film expansion. [c] $TA_{comp-1st}$: trough area during the first film compression. [d] $TA_{expn-1st}$: trough area during the first film expansion.

In Figure 2, time windows #22 and #24 contain the SFG spectra of DPPC-d_{62} in the LE phase (refer to the blue spectra with five peaks). In the LE phase, the angle distribution of the terminal methyl groups of DPPC-d_{62} is not assumed to be a δ function. Therefore, θ and σ factors have to be considered in order to obtain the relationship between I_{ssp} and N. σ is a factor that is difficult to measure; therefore, time windows #22 and #24 are not suitable windows for measuring the interfacial density variation of N. For time window #28, DPPC-d_{62} is in the LC phase for both film compression and film expansion. In the highly packed semicrystalline-like condensed phase, it is reasonable to assume that the DPPC terminal methyl groups have a δ-function angle distribution. Therefore, eq 10 can be used to describe the relationship between I_{ssp} and N. Furthermore, the calculated ratio between the CD_3-SS and the CD_3-AS intensities for the two spectra in Figure 2C are shown to be the same, revealing that the orientation angles of the CD_3 moieties in the two cases are the same. Therefore, the difference between the two BBSFG spectra in Figure 2C is simply due to the variation of interfacial number density, N. Table 2 lists the fitted CD_3-SS intensity (peak area) for time window #28 of the compression and expansion segments. The interfacial density reduction of DPPC-d_{62} is then calculated according to eq 11 and gives a value of 18%.

$$\Delta N = \frac{\sqrt{I_{comp}(CD_3\text{-SS})} - \sqrt{I_{expn}(CD_3\text{-SS})}}{\sqrt{I_{comp}(CD_3\text{-SS})}} \quad (11)$$

Since the trough areas are the same for the compression segment and the expansion segment, this means that there is an 18% loss of DPPC-d_{62} from the interface during film respreading. The second compression isotherm was also investigated at time window #28 with BBSFG. The obtained spectrum (data not shown) was found to be identical to the spectrum of the first expansion in Figure 2C. This indicates that the 18% loss of DPPC-d_{62} during film expansion is irreversible.

Table 2 also lists the trough area for the #28 first expansion segment and its corresponding value for the first compression segment under the same surface pressure of ~29 mN/m. As shown in Table 2, the compression segment has an average trough area of 59 cm^2 and the expansion segment has an average trough area of 37 cm^2. Therefore, there is a 37% trough area reduction after film respreading.

The 18% DPPC interfacial loss and the 37% trough area reduction suggest that there must be additional contributions for the 37% trough area reduction. If we assume that all of the components during respreading have a uniform 18% interfacial loss, then the expansion isotherm would simply shift to the right with a trough area reduction of 18%. This does not occur. The surprisingly large 37% trough area reduction during film respreading clearly indicates that the respreading of DPPC and non-DPPC components in the lung surfactant mixture

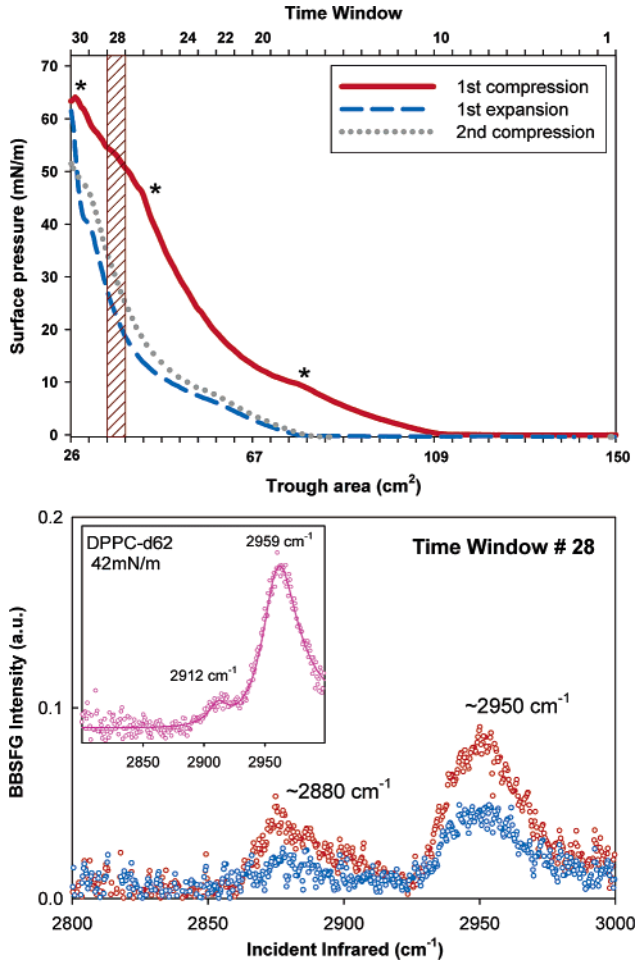

Figure 3. Compression and expansion isotherms of the DPPC-d_{62}−POPG−PA−KL_4 monolayer (top) and ssp BBSFG spectra of DPPC-d_{62} in DPPC-d_{62}−POPG−PA−KL_4 monolayer taken in the C−H stretching region in the time window #28 under N_2-purging conditions (bottom). Red spectrum: spectrum for the first compression isotherm segment. Blue spectrum: spectra for the first expansion isotherm segment. Inset: ssp BBSFG spectrum of DPPC-d_{62} monolayer taken in the C−H stretching region (42 mN/m, LC phase).

is not uniform and a surface refinement process exists during film compression and expansion. The non-DPPC components must be depleted from the interface to a greater extent than DPPC in order to satisfy the observed 37% trough area reduction. Due to this refinement process, the film becomes DPPC-enriched.

The respreading process was also investigated in the C−H stretching region. As shown in Figure 3, the red spectrum corresponds to the first compression and the blue spectrum corresponds to the first expansion. Due to the complexity in this spectral region (POPG, PA, KL_4, and DPPC-d_{62} can all make spectral contributions), no attempt was made to quantify the SFG intensity variation. However, some valuable information is clearly revealed from Figure 3. First, the two spectra (red and blue) are quite different from the nondeuterated headgroup of DPPC-d_{62}, which is shown in the inset, suggesting that the observed SFG signal in the C−H stretching region is primarily from the non-DPPC components. This further means that if DPPC forms different domains from the non-DPPC components during film compression and expansion (this is highly possible based on previous results on similar systems (DPPC/POPG/PA/SP-B) using Brewster angle microscopy[30]), the BBSFG laser system is sensitive to both of the two types domains, DPPC domains and non-DPPC domains. Second, the SFG intensity during the first film expansion does show a substantial decrease as compared with the intensity during the first film compression, corresponding to the interfacial loss of the non-DPPC components.

The depleted surfactants are lost either to the subphase or exist in aggregate form underneath the monolayer in a surface-associated reservoir. The DPPC in the collapse phase, if it remains at the monolayer surface during film expansion, should be in a multilayer (monolayer + bilayer(s)) structure collapse phase.[24,79,80] Due to the opposing orientations of the DPPC monolayers in the bilayer structure, the DPPC underneath the monolayer (in the bilayers) would not produce an SFG signal based on the lack of inversion symmetry SFG selection rule.

The observed DPPC enrichment during film expansion is a consequence of the surface refinement process during film compression. According to the widely accepted selective squeeze-out theory, during film compression of the lung surfactant monolayer, components with a lower collapse pressure (such as POPG) will be selectively squeezed out into the collapse phase first, and due to its high collapse pressure, DPPC will be squeezed out into the collapse phase last.[2,81,82] The observed refinement process in this study results in a DPPC-enriched film at the air−water interface and a non-DPPC component enriched collapse phase, consistent with the squeeze-out theory. The data presented here reveals a 2-fold effect of the selective squeeze-out theory on the lung surfactant function. On one hand, the selective squeeze-out process helps form a DPPC-enriched film during compression, which is beneficial to the attainment of the near-zero surface tension. On the other hand, a non-DPPC component-enriched collapse phase during compression is produced and consequently causes inefficient respreading of the non-DPPC components during film expansion.

It is thought that non-DPPC components such as phosphatidylglycerols and proteins are needed to facilitate the respreading of DPPC.[2,5] This statement emphasizes the importance of the respreading of the DPPC component but neglects the importance of the respreading of the non-DPPC components. The present study indicates that the interfacial loss of non-DPPC components in endogenous and exogenous lung surfactant will be significant during film compression and expansion. Implicated from this study, the respreading of non-DPPC components should be considered equally as important as the DPPC respreading in the design of replacement surfactants.

Conclusion

A real-time broad bandwidth sum frequency generation spectroscopy investigation was performed on a lung surfactant monolayer containing DPPC-d_{62}, POPG, PA, and KL_4. The interfacial loss of DPPC-d_{62} during film respreading was directly quantified for the first time. Spectroscopic evidence along with compression−expansion isotherm data further revealed that the respreading of DPPC and non-DPPC components in the lung surfactant mixture are not uniform and a surface refinement process exists during film compression and expansion. This refinement process results in a DPPC-enriched monolayer after film respreading. Molecular level evidence from this study reveals

(79) Ries, H. E.; Swift, H. *Langmuir* **1987**, *3*, 853.
(80) Birdi, K. S.; Vu, D. T. *Langmuir* **1994**, *10*, 623.
(81) Goerke, J.; Clements, J. A. In *Handbook of Physiology: The Respiratory System*; Mackelm, P. T., Mead, J., Eds.; American Physiology Society: Washington, 1986; Vol. III.; p 247.
(82) Keough, K. M. W. In *Pulmonary Surfactant: From Molecular Biology to Clinical Practice*; Robertson, B., Van Golde, L. M. G., Batenburg, J. J., Eds.; Elsevier: Amsterdam, 1992; p 109.

that the refinement, postulated by the squeeze-out theory, is quantifiable and significant.

Acknowledgment. We acknowledge the Arnold and Mabel Beckman Foundation for funding this research through a Beckman Young Investigator Award.

Supporting Information Available: Respreading experiments performed under ambient atmospheric conditions are shown in Figures S1, S2, and S3 and Table S1. This material is available free of charge via the Internet at http://pubs.acs.org.

LA061476K